Journal of Magnetism and Magnetic Materials 326 (2013) 235–239

Contents lists available at SciVerse ScienceDirect

Journal of Magnetism and Magnetic Materials

journal homepage: www.elsevier.com/locate/jmmm

Letter to the Editor

Origin of strong magnetic anisotropy in $L1_0$-FeNi probed by angular-dependent magnetic circular dichroism

Masato Kotsugi [a,c,*], Masaki Mizuguchi [b,c], Shigeki Sekiya [b], Masaichiro Mizumaki [a], Takayuki Kojima [b,c], Tetsuya Nakamura [a], Hitoshi Osawa [a], Kenji Kodama [a], Takumi Ohtsuki [a,c], Takuo Ohkochi [a,c], Koki Takanashi [b,c], Yoshio Watanabe [a]

[a] SPring-8/JASRI, 1-1-1 Koto, Sayo, Hyogo 679-5198, Japan
[b] Tohoku University, 2-1-1, Katahira, Aoba-ku, Sendai 980-8577, Japan
[c] Japan Science and Technology Agency (JST), 7 Goban-cho, Chiyoda, Tokyo 102-0076, Japan

ARTICLE INFO

Article history:
Received 24 July 2010
Received in revised form
24 August 2012
Available online 17 September 2012

Keywords:
Magnetic anisotropy
Spin–orbit interaction
Magnetic circular dichroism
$L1_0$-FeNi
Iron meteorite

ABSTRACT

We investigated the origin of strong magnetic anisotropy energy (MAE) in $L1_0$-type ordered FeNi phase by angular-dependent magnetic circular dichroism. Our findings showed that the orbital magnetic moment of Fe has a significant angular dependence that exhibits a maximum value at the [001] direction corresponding perpendicular to the plane. The calculated uniaxial anisotropy energy when considering spin–orbit (SO) interaction shows quantitatively good agreement with the volume MAE. We concluded that the orbital anisotropy in 3d Fe electrons results in the strong MAE in $L1_0$-FeNi and ascribe this to the spin–orbit interaction via structural ordering.

1. Introduction

Magnetic anisotropy energy (MAE) is a key property to improve areal density in widespread applications. A number of studies have been done on $L1_0$-type FePt and/or CoPt ferromagnet for use as a magnetic recording medium or magnetoresistive random access memory [1]. From the ecological viewpoint, a rare-metal-free $L1_0$-ferromagnet composed of abundant Fe and Ni has recently been attracting much attention [2].

Conventionally, $L1_0$-FeNi phase has been made up of a rare ferromagnet derived from iron meteorite or produced by neutron irradiation at high temperature [2–10]. However, the molecular beam epitaxy (MBE) technique has recently opened a new possibility for the synthetic fabrication of single crystalline $L1_0$-FeNi film [11]. The magnetic anisotropy energy of $L1_0$-FeNi is shown as 1.3×10^6 J/m^3. It is entirely larger value compared to common FeNi alloys [5–7], in which permalloy shows magnetic anisotropy energy as -2.5×10^4 J/m^3 [12,13]. In other words, $L1_0$-FeNi is characterized as a hard ferromagnet with strong anisotropy despite the fact that common FeNi alloys are classified as a soft magnet. However, the origin of the curiously strong MAE in $L1_0$-FeNi has not been addressed thus far.

MAE has been commonly explained as extra anisotropy energy caused by a symmetry break in the internal lattice [13–32]. $L1_0$-FeNi is described as an ordered alloy of Fe and Ni with a face-centered tetragonal (fct) superstructure, in which Fe and Ni single atomic layers are alternately laminated in the *c*-axis direction (Fig. 1a) [8]. If we can align its uniaxial anisotropy parallel to the *c*-axis, it would offer the possibility of perpendicular magnetization.

By nature, MAE commonly arises from spin–orbit interaction (SO), which causes the presence of anisotropic orbital moment with respect to the crystal axes, and it consequently leads to the alignment of the spin moment with the orbital moment [14]. The resulting anisotropy of the total magnetic moment is reflected in the dependence of the total energy on the orientation of the magnetic moment. Typical 3d transition metals such as Fe, Co and Ni have weak MAE because the orbital magnetic moment is almost completely quenched by crystal field interactions. However, the situation in an ultra thinfilm or multilayer is different from that of bulk. Due to symmetry breakage, the enhanced anisotropic orbital moments can be predicted in tight binding calculations [14,15] and confirmed experimentally [18–24]. In fundamental bilayer systems, MAE is reported to be strongly enhanced at the interface due to spin–orbit interactions [19,20,24]. The number of interfaces is the same as the number of layers in an $L1_0$-type superstructure, which suggests that spin–orbit interaction is a possible candidate to explain the strong MAE in $L1_0$-FeNi [12].

In this study, we investigated the origin of strong MAE in $L1_0$-FeNi from the viewpoint of electronic spin structure. The study was carried

* Corresponding author at: SPring-8/JASRI, 1-1-1 Koto, Sayo, Hyogo 679-5198, Japan. Tel.: +81 791 58 0833.
E-mail address: kotsugi@spring8.or.jp (M. Kotsugi).

0304-8853
http://dx.doi.org/10.1016/j.jmmm.2012.09.008

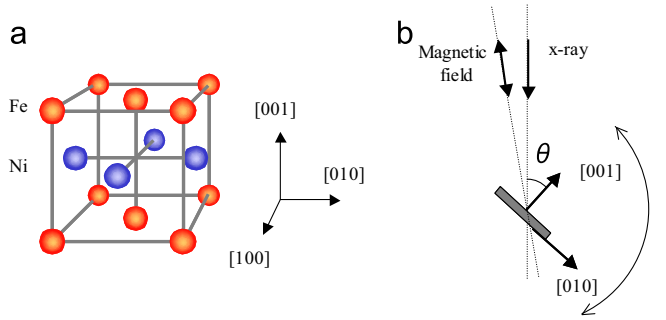

Fig. 1. (a) Lattice structure of $L1_0$-type FeNi superstructure. (b) Experimental geometry of angular-dependent MCD measurement.

out by measuring the angular distribution of orbital moment in connection with lattice structure. We then compared experimental results with theoretical work.

We performed magnetic circular dichroism (MCD) to study the mechanism of the magnetic moment in $L1_0$-FeNi [18–21]. The sum rule was applied to deduce quantitative information from MCD spectra. This rule enables us to obtain the spin and orbital magnetic moments directly from the MCD intensity of the L_3 and L_2 absorption edges, resulting in the element selective determination of magnetic moments in the solids. Although there is still some argument as to the reliability of sum rules, it seems able to extract a reasonable result for 3d transition metals. Angular-dependent MCD enables us to evaluate the anisotropy of the orbital moment that directly informs the contribution of the spin–orbit interaction in MAE [19,22]. Bruno has previously demonstrated a simple perturbation theory arguing that MAE due to spin–orbit interaction is closely connected to the angular distribution of the orbital moment [14]. Measurements were performed for both ordered and disordered FeNi to determine the correlation with the lattice structure.

2. Sample preparation

It has long been thought that the synthesis of $L1_0$-FeNi was not realistic for electromagnetic applications because it could be obtained from natural iron meteorites or by neutron irradiation at high temperature [6,7]. Shima et al. recently succeeded in preparing single crystalline $L1_0$-FeNi films by alternating the deposition of Fe and Ni using the MBE technique [11]. Its fundamental properties are currently being systematically examined to improve MAE [35–40]. For example, the correlation between MAE and lattice structure has been discussed by Mizuguchi et al. [36–38]. Magnetic domain structure was evaluated by Kotsugi et al. [39], and theoretical calculations were carried out [36,40]. Sakamaki et al. also prepared FeNi multilayer using electron bombardment evaporation, but perpendicularly magnetized thick Ni substrate was used and its contribution was not considered [41]. Here, we prepared the $L1_0$-FeNi multilayer with the repetition of 50 times on the non-magnetic substrate to examine true MAE of ordered FeNi mulitilayer itself. In this study, we used a sample with $K_u = 4.8 \times 10^5$ J/m^3 for the MCD measurement.

MBE has a strong advantage in that it can control the deposition rate accurately, and the hetero-epitaxial growth is helpful in fabricating the superstructure of $L1_0$-FeNi. The growth procedure and its structure has been discussed in detail by Mizuguchi et al. [35,36,39]. Here, we briefly describe the sample preparation. A Fe/Ni multilayer was fabricated on a Cu/Au/Fe/MgO substrate using an ultra high vacuum deposition system with independent multiple evaporators. A 1-nm Fe seed layer was deposited on a MgO(001) substrate at 100 °C, then 20 nm of Au was deposited, and finally 50 nm of Cu was deposited at 496.9 °C. These temperatures were optimized for the preparation of atomically flat substrates [35]. In the next step, monoatomic layers of Fe and Ni were alternately deposited on the top. This alternated deposition was repeated 50 times at 187.3 °C. The prepared surface is (001). The thickness was controlled on the basis of values observed by a quartz oscillator. The calibration of the oscillator was carefully controlled by observing the oscillation in reflection high-energy electron diffraction (RHEED) intensity before preparing the multilayer films. The surface structure was monitored by RHEED observation.

The lattice constant of $L1_0$-FeNi was evaluated as $a = 3.65$, $c = 3.59$ Å using X-ray diffraction (XRD) of BL46XU at SPring-8. The superlattice peak was clearly visible and its degree of order was estimated to be 0.38 [36]. Magnetization curve measurements using a superconducting quantum interface device (SQUID) showed that the magnetic anisotropic energy K_u was 4.8×10^5 and 0.6×10^5 J/m^3 for $L1_0$-FeNi and disorder FeNi, respectively.

3. Experiment

The MCD measurement was performed at the L absorption edge of Fe and Ni using BL25SU of SPring-8 [33,34]. The relationship between magnetic moment and magnetic anisotropy was studied by observing the dependence of MCD on the incident angle of synchrotron radiation [18,19]. By defining the polar angle θ as the angle between the synchrotron radiation and the [001] direction of the sample, the θ was varied from the out-of-plane [001] direction to the in-plane [010] direction. An external magnetic field was applied to magnetize the specimen using an electromagnet with a longitudinal geometry. The direction of the external magnetic field was essentially parallel to the incident beam, which was fixed at 10° due to the experimental apparatus. The applied field of 1.9 T was large enough to saturate the sample magnetization. The MCD signal was collected using the total electron yield method. We used the helicity reversal technique with a kicker magnet to obtain accurate statistics from the MCD spectra, in which the zero line is well below the order of 0.1% with respect to the main peak. Experiment was performed at room temperature. The magnitudes of the orbital magnetic moment and spin magnetic moment were obtained by applying the sum rule to MCD spectra [18]. Applied sum rule was typical analytical procedures. We subtracted XAS spectra by arctangent step function, and we integrate the XAS and MCD spectra to derive orbital and spin magnetic moments. We adopt 717 eV for the intermediate energy of $L_{2,3}$ edge of Fe and 780 eV for the energy of post edge of Fe, we also adopt 865 eV for the energy of $L_{2,3}$ edge of Ni and 920 eV for the energy of post edge of Ni in this paper. To estimate error bars, we set the margin of ± 3 eV for the intermediate energy of $L_{2,3}$ edge and ± 5 eV for the post edge. The hole numbers were adopted to be 3.39 and 1.5 for Fe and Ni, respectively, from literature [18], and it is not included in the error bars. Data acquisition error was about 0.1%. We estimated error bars by substituting photon energy and considering its margin. Typical error bar was about 12% for orbital magnetic moment, and about 3% for spin magnetic moment.

4. Results and discussion

The MCD experiment for Fe and Ni L edges was performed while varying the incident angle from -10 to 80°. The measurement was repeated for $L1_0$- and disordered-FeNi. Fig. 2 shows MCD spectra obtained from $L1_0$-FeNi with the incident angle of 0° as an example. The sign and shape of the MCD spectra is entirely

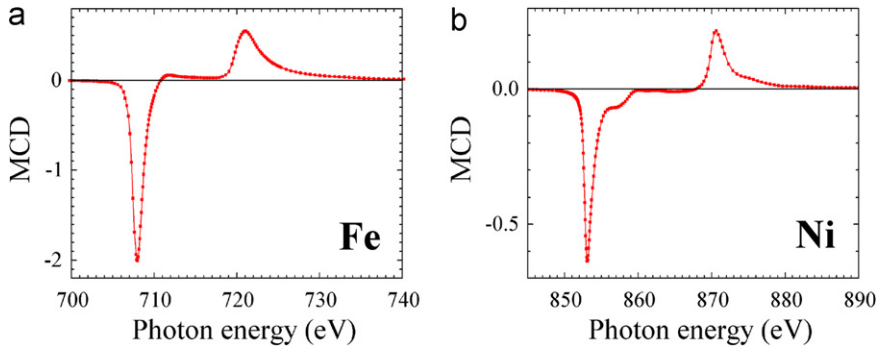

Fig. 2. MCD spectra observed for $L1_0$-FeNi with the incident angle of 0°. Spectra were obtained for Fe L edge (a) and Ni L edge (b). These statistics are accurate enough to use sum-rule analysis.

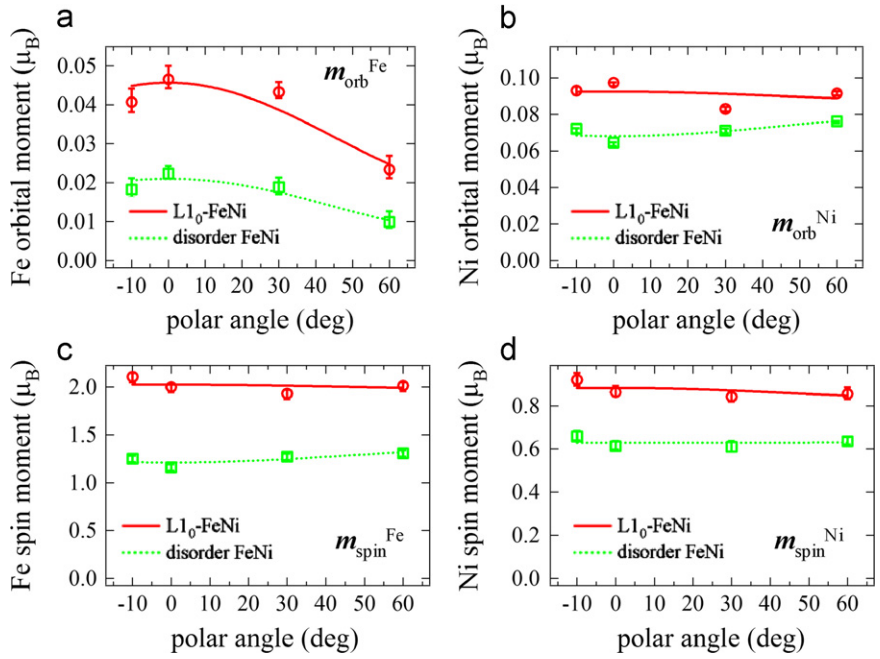

Fig. 3. Angular distribution of orbital moment and spin moment of Fe and Ni for $L1_0$- and disordered-FeNi analytically obtained by sum rule. A clear angular dependence is exhibited in the orbital moment of Fe. The others show no clear angular distribution. The improvement in the Fe orbital moment results in an increased MAE through the spin–orbit interaction.

clear, and there are no complex shoulders or satellites. This behavior is identical to common metallic Fe and Ni MCD spectra, meaning sum-rule analysis might be applicable.

Fig. 3 shows the angular dependence of the orbital and spin magnetic moments of Fe and Ni for $L1_0$- and the disordered-FeNi alloy, which was analytically obtained from the MCD spectra using the sum rule. The angular distribution in the Fe orbital magnetic moment shows a clear and strong angular dependence (Fig. 3a), but the Ni orbital magnetic moment displays an unclear angular distribution (Fig. 3b). The spin magnetic moments of both Fe and Ni show no angular dependence, as shown in Fig. 3c and d. The orbital term of Fe had a maximum value near 0° of the polar angle, which corresponded to the [001] direction. Such anisotropic behavior in the Fe 3d orbital magnetic moment has a positive correlation with the strong MAE in $L1_0$-FeNi enhancing to the [001] direction. Strictly speaking, spin moment and effective spin moment should be treated as distinct. Angular dependence of magnetic dipole term T_z was discussed by the first principle calculation of Oguchi et al. [42]. They indicated that T_z shows obvious angular distribution at the surface, but it rapidly decreases at more than 3 ML. Our system (100 ML) or the penetration depth of the photoelectron (about 5 nm) is much thicker than 3 ML. Therefore, the contribution of T_z at surface would be negligibly small, and we here consider T_z is isotropic.

Bruno has predicted a close connection between the MAE and the orbital moment from transition metal monolayers of Fe, Co and Ni. The angular distribution in orbital moment can be expressed by an ellipsoidal function as follows [14,20,24].

$$m_{\mathrm{orb}} = m_{\mathrm{orb}}^{\perp} \cos^2\theta + m_{\mathrm{orb}}^{\parallel} \sin^2\theta$$

and the uniaxial anisotropy of orbital moment is expressed as

$$\Delta m_{\mathrm{orb}} = m_{\mathrm{orb}}^{\perp} - m_{\mathrm{orb}}^{\parallel}$$

Perpendicular and parallel orbital components are derived from the fitting on the experimentally obtained orbital moment, resulting in $\Delta m_{\mathrm{orb}}^{Fe} = -0.028$ and $\Delta m_{\mathrm{orb}}^{Ni} = -0.005$ for the orbital moment of Fe and Ni in $L1_0$-FeNi, as shown in Table 1. Bruno has shown in a simple perturbation theory based on tight binding approximation that the MAE in a uniaxial system is caused by the spin–orbit interaction $\xi l \cdot s$, which is directly connected to the anisotropy of the orbital moment, and for a more than half-filled d shell. In a simple model, a relation between the orbital magnetic

Table 1
Orbital anisotropy and extracted MAE for Fe and Ni: spin–orbit interaction was derived from simple perturbation theory by Bruno based on tight binding approximation.

Sample	$\Delta m_{orb}(\mu_B)$	ΔE_{SO} (μev/unit cell)	MAE (μev/unit cell)
$L1_0$-FeNi			
Fe	−0.028	160	142
Ni	−0.005		
Disorder FeNi			
Fe	−0.014	16	18.7
Ni	0.011		

moment m_{orb} and the spin–orbit energy E_{SO} was derived.

$$\Delta E_{SO} = \frac{G}{H}\frac{\xi}{4\mu_B}\Delta m_{orb}$$

where G and H are density-of-state integrals. G/H becomes 1 if the exchange splitting is larger than band width. For 3d transition metals, G/H is roughly estimated as about 0.2 or smaller. ξ is the spin–orbit constant, and is of the order of 0.05 eV we used [14,20,24]. This is small compared with the 3d band width and therefore justifies perturbative treatment. Wang et al. reported additional terms related with the magnetic dipole term T_z [43]. van der Laan also argued an important notice that MAE is proportional to orbital moment only when the majority band is completely filled [44]. Since this equation is approximate case for Fe and Ni, we adopted this proportional formula here. Thus, we obtain $\Delta E_{SO}^{Fe} = 67.9$ μeV/atom and $\Delta E_{SO}^{Ni} = 12.1$ μeV/atom for Fe and Ni, respectively. The corresponding total ΔE_{SO} is about 160 μeV per unit cell. The volume anisotropy was obtained as $K_u = 4.8 \times 10^4$ J/m^3 and the corresponding $\Delta E_{SO} = 142$ μeV per unit cell by adopting the lattice constant of $a = 3.64$ Å and $c = 3.59$ Å. These values show good agreements and consequently, the large MAE in $L1_0$-FeNi is ascribed to the anisotropy in the orbital moments of Fe and Ni through the spin–orbit interaction. The tight-binding approximation adequately describes the strong MAE in $L1_0$-FeNi.

For disordered FeNi, orbital anisotropy is given as $m_{orb}^{Fe} = -0.014\ \mu_B$ and $m_{orb}^{Ni} = 0.011\ \mu_B$, resulting in a spin–orbit interaction of $\Delta E_{SO} = 16$ μeV. The disordered FeNi shows a negative Δm_{orb} in the Ni moment, which is balanced out in the Fe, thus resulting in the low K_u in the disordered FeNi phase. It also shows good agreement with the volume anisotropy of 18.7 μeV per unit cell ($K_u = 0.6 \times 10^5$ J/m^3).

Finally, we concluded that the large MAE in the $L1_0$-FeNi phase can be directly ascribed to the spin–orbit interaction. We also note that this result is consistent with theoretical calculation by Miura et al. [45]. The Fe orbital moment shows strong angular dependence with a maximum value at the [001] direction corresponding to out-of-plane. The orbital anisotropy of Fe 3d electrons mainly results in the large MAE via spin–orbit coupling. Controlling the orbital magnetic moment at the interface will play a key role in further improvements to MAE in $L1_0$-FeNi.

Acknowledgments

This work was partially supported in part by a Grant-in-Aid for Scientific Research (Young scientist (B) 17740198, 19740210) and a Grant-in-Aid for Scientific Research in Priority Area "Creation and control of spin current" and by a grant from the Global COE program "Materials Integration International Center of Education Research" from the Ministry of Education, Culture, Sports, Science and Technology, Japan. The MCD experiment was carried out under the approval of SPring-8 (Proposals: 2007B1258 and 2008A2056). The MCD analysis was supported by Industry-Academia Collaborative R&D Programs of Japan Science and Technology Agency.

References

[1] T. Shima, K. Takanashi., Handbook of Magnetism and Advanced Magnetic Materials, 2007, p. 2306.
[2] M. Kotsugi, C. Mitsumata, H. Maruyama, T. Wakita, T. Taniuchi, K. Ono, M. Suzuki, N. Kawamura, N. Ishimatsu, M. Oshima, Y. Watanabe, M. Taniguchi, Applied Physics Express 3 (2010) 13001.
[3] J.F. Albertsen, G.F. Jensen, J.M. Knudsen, Nature 273 (1978) 453.
[4] R.S. Clarke, E.R.D. Scott, American Mineralogist 65 (1980) 624.
[5] J.F. Albertsen, Physica Scripta 23 (1981) 301.
[6] L. Néel, J. Pauleve, R. Pauthenet, J. Laugier, D.J. Dautreppe, Journal of Applied Physics 35 (873) (1964) 873.
[7] J. Pauleve, A. Chamberod, K. Krebs, A. Bourret, Journal of Applied Physics 39 (1968) 989.
[8] T. Horiuchi, M. Igarashi, F. Abe, T. Mohri, Calphad 26 (2002) 591.
[9] M. Kotsugi, T. Wakita, T. Taniuchi, H. Maruyama, C. Mitsumata, K. Ono, M. Suzuki, N. Kawamura, N. Ishimatsu, M. Oshima, Y. Watanabe, M. Taniguchi, IBM Journal of Research and Development 55 (2011) 13.
[10] M. Kotsugi, T. Wakita, N. Kawamura, T. Taniuchi, K. Ono, M. Suzuki, M. Takagaki, M. Taniguchi, M. Oshima, N. Ishimatsu, H. Maruyama, Surface Science 601 (2007) 4764.
[11] T. Shima, M. Okamura, S. Mitani, K. Takanashi, Journal of Magnetism and Magnetic Materials 310 (2007) 2213.
[12] S. Chikazumi, Handbook of Magnetic material, vol. 782, Asakura-shoten, Tokyo, 1975, pp. 324–327.
[13] S. Chikazumi, Physics of Ferromagnetism, vol. II, Shyokabo, Tokyo, 1984, p. 21.
[14] P. Bruno, Physical Review B 39 (1989) 865.
[15] B.T. Thole, P. Carra, F. Sette, G. van der Laan, Physical Review Letters 68 (1992) 1943.
[16] P. Carra, B.T. Thole, M. Altarelli, X. Wang, Physical Review Letters 70 (1993) 694.
[17] H.A. Dürr, G. van der Laan, Physical Review B 54 (1996) R760.
[18] J. Stöhr, H. König, Physical Review Letters 75 (1995) 3748.
[19] D. Weller, Y. Wu, J. Stöhr, M.G. Samant, B.D. Hermsmeier, C. Chappert, Physical Review B 49 (1994) 12888.
[20] D. Weller, J. Stöhr, R. Nakajima, A. Carl, M.G. Samant, C. Chappert, R. Megy, P. Beauvillain, P. Veillet, G.A. Held, Physical Review Letters 75 (1995) 3752.
[21] C.T. Chen, Y.U. Idzerda, H.-J. Lin, N.V. Smith, G. Meigs, E. Chaban, G.H. Ho, E. Pellegrin, F. Sette, Physical Review Letters 75 (1995) 152.
[22] T. Koide, H. Miyauchi, J. Okamoto, T. Shidara, A. Fujimori, H. Fukutani, K. Amemiya, H. Takeshita, S. Yuasa, T. Katayama, Y. Suzuki, Physical Review Letters 87 (2001) 257201.
[23] N. Nakajima, T. Koide, T. Shidara, H. Miyauchi, H. Fukutani, A. Fujimori, K. Ito, T. Katayama, M. Myvly, Y. Suzuki, Physical Review Letters 81 (1998) 5229.
[24] W. Kuch, J. Gilles, S.S. Kang, S. Imada, S. Suga, J. Kirschner, Physical Review B 62 (2000) 3824.
[25] J. Thomassen, F. May, B. Feldmann, M. Wuttig, H. Ibach, Physical Review Letters 69 (1992) 3831.
[26] Dongqi Li, M. Freitag, J. Pearson, Z.Q. Qiu, S.D. Bader, Physical Review Letters 72 (1994) 3112.
[27] D. Qian, X.F. Jin, J. Barthel, M. Klaua, J. Kirschner, Physical Review Letters 87 (2001) 227204.
[28] K.L. Man, M.S. Altman, H. Poppa, Surface Science 480 (2001) 163.
[29] B. Lazarovits, L. Szunyogh, P. Weinberger, B.U. jfalussy, Physical Review B 68 (2003) 024433.
[30] C. Klein, R. Ramchal, A.K. Schmid, M. Farle, Physical Review B 75 (2007) 193405.
[31] J. Choi, J. Wu, C. Won, Y.Z. Wu, A. Scholl, A. Doran, T. Owens, Z.Q. Qiu, Physical Review Letters 98 (2007) 207205.
[32] R. Ramchal, A.K. Schmid, M. Farle, H. Poppa, Physical Review B 69 (2004) 214401.
[33] S. Suga, S. Imada, A. Yamasaki, S. Ueda, T. Muro, Y. Saitoh, Journal of Magnetism and Magnetic Materials 233 (2001) 60.
[34] T. Nakamura, T. Muro, F.Z. Guo, T. Matsushita, T. Wakita, T. Hirono, Y. Takeuchi, K. Kobayashi, Journal of Electron Spectroscopy and Related Phenomena 144 (2005) 1035.
[35] M. Mizuguchi, S. Sekiya, K. Takanashi, Journal of Applied Physics 107 (2010) 09A716.
[36] T. Kojima, M. Mizuguchi, T. Koganezawa, K. Osaka, M. Kotsugi, K. Takanashi, Japanese Journal of Applied Physics 51 (2012) 010204.
[37] M. Mizuguchi, T. Kojima, M. Kotsugi, T. Koganezawa, K. Osaka, K. Takanashi, Journal of the Magnetics Society of Japan 35 (2011) 370.
[38] T. Kojima, M. Mizuguchi, K. Takanashi, Journal of Physics: Conference Series 266 (2011) 012119.
[39] M. Kotsugi, M. Mizuguchi, S. Sekiya, T. Ohkouchi, T. Kojima, K. Takanashi, Y. Watanabe, Journal of Physics: Conference Series 266 (2011) 012095.

[40] C. Mitsumata, Y. Kota, A. Sakuma, M. Kotsugi, Journal of the Magnetics Society of Japan 35 (2011) 52.
[41] M. Sakamaki, K. Amemiya, Applied Physics Express 4 (2011) 073002.
[42] T. Oguchi, T. Shishidou, Physical Review B 70 (2004) 024412.
[43] D.S. Wang, R. Wu, A.J. Freeman, Physical Review B 47 (1993) 14932.
[44] G. van der Laan, Journal of Physics: Condensed Matter 10 (1998) 3239.
[45] Y. Miura, S. Ozaki, Y. Kuwahara, M. Tsujikawa, K. Abe, M. Shirai, Condensed Matter > Materials Science, arXiv:1209.5003.